We are IntechOpen, the world's leading publisher of Open Access books Built by scientists, for scientists

6,900
Open access books available

185,000
International authors and editors

200M
Downloads

Our authors are among the

154
Countries delivered to

TOP 1%
most cited scientists

12.2%
Contributors from top 500 universities



WEB OF SCIENCE™

Selection of our books indexed in the Book Citation Index in Web of Science™ Core Collection (BKCI)

Interested in publishing with us?
Contact book.department@intechopen.com

Numbers displayed above are based on latest data collected.
For more information visit www.intechopen.com



Provisional chapter

Assessment and Prediction of Evapotranspiration Based on Scintillometry and Meteorological Datasets

Antonin Poisson, Angel Fernandez, Dario G. Gomez, Régis Barillé and Benoit Chorro

Additional information is available at the end of the chapter

Abstract

Two methods are used for estimating the evapotranspiration (ET) rate: scintillometry and meteorological measurements using the FAO-PM56 model with the reference evapotranspiration for the crop (ETO) and the specific coefficient (Kc) for corn at its stage development. Measurements were done on a field with homogeneous corn crop at the stage of 3 months before the final harvest (65 % of maximum plant growth). The two methods are compared with environmental parameters to determine the most influential on the final result of ET.

A coefficient of 0.78 is found between the two methods resulting of an underestimation of the evapotranspiration values with FAO.

The sensitivity for the two measurements are compared in order to determine how sensitive the output calculation of evapotranspiration could be with respect to the calculation elements which are subject to uncertainty of variability in the input environmental parameters. The scintillometer uncertainty is lower than the FAO-56 uncertainty.

Finally, a model based on an artificial neural network (ANN) forecasting ET is developed in order to anticipate the necessary action for water management. It leads to the conclusion that scintillometry is more able to predict evapotranspiration on short and medium time than the FAO-PM56 method.

Keywords: evapotranspiration, FAO-PM56, scintillometry, artificial neural network

1. Introduction

Water resources are highly influenced by the hydrologic cycle and play a role in the agriculture economic development. However, as it is shown by the intergovernmental panel on climate change report [1], the phenomenon of changing climate is set way to exacerbate an already

INTECH
open science | open minds

© 2018 The Author(s). Licensee InTech. This chapter is distributed under the terms of the Creative Commons Attribution License (http://creativecommons.org/licenses/by/3.0), which permits unrestricted use, distribution, and reproduction in any medium, provided the original work is properly cited. CC BY

serious situation of water supply for various users. Agricultural production will be one of the sectors most vulnerable to climate change and variability. The water budget must now be shared with agriculture, urban use, industry, recreation and livestock watering; the future will be seeing an increasing competition for water. Spatial and temporal changes in precipitation and temperature patterns will have an impact on the viability of dry land farming and therefore necessitate irrigation where rainfall was previously adequate. Efficiency improvement in irrigation lies among the key strategies for saving more water and promote a sustainable intensification of agriculture when water scarcity becomes a major constraint to production [2]. Nevertheless, irrigation water for crops is globally the major consumptive use of water resources. Due to the above-mentioned challenges, it is important to improve the management of agricultural water, which would involve the accurate estimation of consumptive uses. One of the techniques is the measurement of evapotranspiration which is a major component of the hydrologic cycle. Evapotranspiration (ET) is an essential component of the water balance, and it is a significant consumptive witness of precipitation and water applied for irrigation of cropland [3]. ET can help for highly efficient management of water uses in agriculture and set up real water-saving systems.

Basically, ET includes two processes: One is evaporation and the second is transpiration. The latter is the process of removing water from vegetation or any other moisture containing living surface. Evapotranspiration includes two processes. During the plant growth, the water stored in the soil is taped and transferred in the atmosphere. Transpiration is the evaporation of water in the vascular system of plants through the leaf stomata when they open and close controlled by their guard cells. Based on this bio-physical process, transpiration involves a living organism and its tissues. ET is then the process, whereby water originating from a wide range of sources is transferred from the soil compartment and/or vegetation layer to the atmosphere. ET is the largest outgoing water flux from the Earth's surface and accurately quantifying ET is critical for the development of crop cultures in an increasing drier environment, and it can contribute to a greater understanding of a range of agricultural ecosystem processes. ET is particularly fundamental when dealing with water resource management issues such as irrigation water or water reserve management [4]. ET cannot be directly measured but it has to be estimated by monitoring the exchange of energy/water above the vegetated surface (remote sensing) or as a residual term of the hydrological balance.

Several methods are currently used to measure and estimate ET: One of them is the lysimeter method or soil water budget. That method may be accurate but lysimeters are expensive, and the extent of their measurement is localized (i.e., they provide data for a very small area compared to the field surface, so it can only be used in field locations). Another one uses micrometeorological data to compute ET. A widely used approach by these data is the FAO-24 and by extension the FAO-56 procedure, based on ET_0 and Kc [5]. ET acquisition can be obtained with different instruments at the scale of: the leaf (porometer), an individual plant (i.e., sapflow, lysimeter), the field scale (i.e., field water balance, Bowen ratio, scintillometer) and the landscape scale (i.e., eddy correlation and catchment water balance) [6]. The flux measurement of micro-meteorological station can only represent the value in a point or a limited area (several meters to several hundred meters). However, a scintillometer can measure averaged sensible heat fluxes in a distance of 500m to 10 km, which is an average of time

and space. The measurement scale of a scintillometer is matching to the grid scale of atmospheric model and the pixel scale of remote sensing, as a result. This advantage promotes the development of scintillometers in recent years [7].

The objective of this work is to compare two methods used for estimating ET rate: scintillometry and meteorological measurements with the FAO-PM56 model based on ET_0 and Kc with the reference evapotranspiration for the crop (ET_0) and the specific crop coefficient for the cultivation type at its stage development (Kc). Also, it is compared how the final result of ET, calculated with the two different measurements, can be more sensible to different environmental parameters. The sensitivity of the two methods is calculated and the influence of the main environmental parameters on the accurate values of ET.

In order to anticipate the necessary action for water management, a model to forecast ET based on an artificial neural network (ANN) is developed. In recent years, ANN models have become extremely popular for prediction and forecasting in a number [8, 9] of domains, including finance, power generation, medicine, water resources and environmental science [8, 9]. The evapotranspiration process calculated with the FAO-PM56 and scintillometry data is a nonlinear process. ANN models are quite appropriate for the simulation of ET leading to good results.

The predicted output final results are compared for two different input parameters of ET calculated with scintillometry and micro-meteorology data. The final goal of this study is to find which input data can be reliable to obtain ET forecast performances. Moreover, the optimal number of predicted days to obtain a correct final performance and the optimal number of input days of data to obtain a correct prediction are tested.

2. Materials and methods

2.1. Site description

The study was carried out in the west part of France near to Niort (France). The site of the intercomparison of evapotranspiration measurements is located in the village of Sainte Soline (contained near 46°15′27.7″N—0°02′32.0″E**)** (**Figure 1**), and the area's elevation is 117—145 m above the sea level. According to data from the Meteorologisk Institute, the daily mean temperatures vary significantly from 5°C in January to 26°C in July. The average days with precipitation per month are 12 days in January and 6 days in August. Mean annual rainfall is 6.4 mm and is distributed relatively evenly across all months. The dominant wind directions are from the south-west and west-south-west and north. The site consists of a field with homogeneous corn crop. Corn corresponds to plants DKc 4590. Corn was planted in April, and the measurements were made at the stage of 4 months (almost 5 months) after planting corresponding to about 65% of maximum plant growth and to 3 months (just before) of the final harvest.

The soil type is clay, and the typical porosity of this soil type is about 0.30 $m^3\ m^{-3}$ with grain size <0.002 mm.



Figure 1. Location map of the measurements during the summer time and contained between 46°15′27.7″N and 0°02′32.0″E.

2.2. Measurement description

The scintillometer provides the opportunity to obtain surface fluxes of sensible heat across a distance of several kilometers and over a heterogeneous landscape [10]. As shown by different authors, it is feasible to use the scintillometer for estimating area-averaged sensible heat flux <λE> ($\lambda E = R_n - G - H$) as the residual term of the energy balance equation, providing estimations of area-average available energy ($\lambda E = R_n - G$) with E the sensible heat flux, λ the latent heat, R_n the net radiation and G the soil heat flux [11]. The transmitter and receiver of the scintillometer system were installed at opposite edges of the field, and the electromagnetic radiation was transmitted across the field. Scintillometry measurements are based on the propagation of electromagnetic waves in atmosphere and the measurement of its disturbance by atmospheric turbulence. The turbulence effect induces laser beam fluctuations leading to beam scintillations, wanderings as a result of random fluctuations of atmospheric temperature and refractive index changes, humidity, pressure and their interactions. A scintillometer measures the normalized variance of radiation intensity.

The scintillometer set up consists of an emitter and a receiver, placed in front of each other at the distance L, where the measurement is made.

The scintillometer consists in an emitter and a receiver. The emitter includes a continuous laser and a pair of lenses to collimate the beam over the optical path. The laser wavelength used is 532 nm with an average power of 70 mW. The output beam of the laser beam is expanding

with a Galilean telescope with chosen lenses. The beam is then collimated over a long distance typically for distances less than 200 m. The optical system has a plano-convex lens with a focal length of 15 mm after the laser output. In order to have a magnification of 5 a second plano-convex lens with a 300 mm, focal length is placed 30 cm from the first one. Finally, at the output of the emitter, the diameter of the beam is then 2 cm. A Rayleigh range of around 142 m for the output collimated beam is obtained with the pair of lenses. The receiver uses a Galilean telescope to recollect the light. A position sensing detector sensor with lateral effect (Duo lateral PSD) defined by the size of the light spot is used as the detector and provide position informations only up to the point where the edge of the spot reaches the gap. The lateral effect position sensing detector is 100 mm^2 (10 mm x 10 mm). Additionally, it is important to enlarge the beam with a combination of two lenses enabling a magnification of 5 in order to have a sufficiently large measurement field. The first lens is plano-convex with a focal length of 60 mm, and the second is plano-concave with a focal length of −24 mm. The two lenses are separated with a distance of 86 mm. For stability during the measurements, all the optical components are mounted on a metal board. The electronic system includes an electronic system for data acquisition and a remote interface with the operators. The scintillometer is a stand-alone system with batteries, solar cells and a communicating system to send data. That device has been built for simultaneously recording both random intensity fluctuations and displacement of the beam centroid (wandering).

The scintillometer provides a measurement of the structure parameter for the refractive index (C_n^2) along the optical path. The structure parameter of the refractive index of air C_n^2 was calculated from the natural logarithm of the intensity of light (I)

$$\sigma_{lnA}^2 = 0.031 k^{7/6} L^{11/6} C_n^2 \tag{1}$$

where L is the beam path length (m), k is the optical wave number (m^{-1}) defined for the wavelength λ as: $k = 2\pi/\lambda$ and $\sigma_{lnA}^2 = \frac{1}{4} ln\left(1 + \sigma_I^2\right)$ with σ_I^2 defined as: $\sigma_I^2 = \langle I^2 \rangle - \langle I \rangle^2 / \langle I \rangle^2$. So the representative value of C_n^2 is 10^{-15} to $10^{-18} m^{-2/3}$.

The parameters such as temperature (T), humidity (q) and pressure (P) generate fluctuations in the refractive index of air C_n^2; however, as the proportion of pressure is very small, this value is always neglected. In the range of visible and near-infrared region, the temperature is the main parameter, assuming that temperature and humidity are perfectly correlated, the structure parameter C_n^2 can be related to the structure parameter $C_T{}^2$ for temperatures by [12]

$$C_T^2 = C_n^2 \left(\frac{0.78 \times 10^{-6} P}{T^2} \right)^{-2} \left(1 + \frac{0.03}{\beta} \right)^{-2} \tag{2}$$

where β is the Bowen ratio, which connect temperature and humidity by the ratio of sensible flux and latent heat flux ($\beta = H/\lambda E$). The second term in brackets is a correction for the effects of humidity. C_T^2 is given in ($K^2.m^{-2/3}$).

The sensible heat flux can be derived from the Monin-Obukhov Similarity Theory (MOST) [13] when C_T^2 is known. This value depends on the stability parameter $\zeta = (z_{scin} - d)/L$, where z_{scin} and d are the effective height of the scintillometer above the surface and the displacement height, respectively. L_O is the Monin-Obukhov length (m) given by

$$L_O = \frac{u^2 T}{kgT^*} \tag{3}$$

with $k = 0.41$ is the von Karman constant, $g = 9.81\ ms^{-2}$ the gravity and $u^*\left[m.s^{-1}\right]$ the friction velocity, given by

$$u^* = \frac{ku}{ln\left(\frac{z-d}{z_0}\right) - \psi} \tag{4}$$

where u is the wind speed, $z_0 = 0.1h_{veg}$ is the surface roughness length and ψ is the stability correction function depending on z/L_O. The universal function ψ is only related to the atmosphere stability and has different expression under stable and unstable conditions [14]. The sensible heat flux H_{scin} can be then computed iteratively as follows

$$H_{scin} = -\rho c_p u^* T^* \tag{5}$$

where ρ and c_p are the density and specific heat capacity of the air, respectively. During the iteration, β is calculated using H_{scin}, net radiation (R_n) and soil heat flux (G)

$$\beta = \frac{H_{scin}}{R_n - G - H_{scin}} \tag{6}$$

The value of the latent heat flux (evapotranspiration) can then be calculated as the residual of the energy balance

$$\lambda_v E_{scin} = R_n - G - H_{scin} \tag{7}$$

where $R_n\ \left[\mathrm{W.m^{-2}}\right]$ is the net radiation and $G\ \left[\mathrm{W.m^{-2}}\right]$ is the soil heat flux. Additional data of temperature, pressure and humidity are necessary to compute the characteristic parameters of the latent heat flux. More specific information on the described approach is found in Ref. [15].

Simultaneously, the air and ground temperature were measured with a thermistor device and linked to the transmission system. The humidity was measured with a capacitive sensor and the wind speed with an anemometer. All the data were collected by a data acquisition electronic system, based on an Arduino board [16], and sent as text files by a modem through the GPRS network and a SIM card.

2.3. Estimation of evapotranspiration based on micro-meteorological datasets

In addition to the data provided by the scintillometer, estimation of the reference crop evapotranspiration ET_0 can be based on energy balance schemes and the Penman-Monteith

(FAO-PM56) method [17, 18]; they are used to assess ET_0 from meteorological variables. The reference crop evapotranspiration or reference evapotranspiration, denoted as ET_0 or ET_{ref}, is the estimation of the evapotranspiration from a "reference surface." The reference surface is a hypothetical grass reference crop with an assumed crop height of 0.12 m, a fixed surface resistance of 70 S/m and an albedo of 0.23. In the reference evapotranspiration definition, the reference surface is specifically defined as the reference crop, and this crop is assumed to be free of water stress and diseases with a fixed surface resistance of 70 S/m. This reference surface has grass with a uniform height, normally growing and totally covering the ground. The soil surface is moderately dry resulting from about a weekly irrigation frequency.

The FAO Penman-Monteith method has been reported as providing consistent ET_0 values in many regions and climates [19]; it has long been accepted worldwide as an excellent ET_0 estimator when it is compared with other methods. The application of ET_0 models with fewer meteorological variable requirements is recommended under situations where weather data sets are incomplete. Those values are multiplied by an empirical crop coefficient to obtain the ET from the crop (ET_c). The crop coefficient accounts for the difference between the standard surface and the crop. Reference ET is expressed in units of depth time^{-1}, for example, mm day^{-1}. It is a climatic parameter expressing the evaporative power of the atmosphere at the given space and time coordinates [20].

Empirical formulas have been developed to estimate solar radiation using some normal observations from meteorological stations, such as maximum and minimum temperatures, sunshine hours, cloud, precipitation, latitude and elevation. FAO Penman-Monteith procedures allow applying the method when only air temperature and wind speed are available. In these methods, saturation vapor pressure and actual vapor pressure were estimated from T_{max} and T_{min}, as recommended by Allen et al. [22] for situations where air humidity data are lacking or are of questionable quality.

The standard FAO Penman-Monteith method is based on the following equation [21]

$$ET_0 = \frac{0.408\Delta(R_n - G) + \gamma\left(\frac{0.37}{(T_a + 273)}\right)u_2(e_s - e_a)}{\Delta + \gamma(1 + 0.34u_2)} \tag{8}$$

where ET_0 represents the hourly reference evapotranspiration (mm h^{-1}), Δ represents the slope vapor pressure curve (kPa.°C^{-1}), R_n is the net radiation at the crop surface (MJ m^{-2} h^{-1}), G indicates the soil heat flux density (MJ.m^{-2}.h^{-1}), γ is the psychrometric constant (kPa.°C^{-1}), T_a is the mean air temperature at 2 m height (°C), u_2 is the mean hourly wind speed at 2 m height (m s^{-1}), e_s defines the saturation vapor pressure at air temperature T_a (kPa) and e_a indicates the actual vapor pressure (kPa). All meteorological data required by the equation were collected by the aid of a weather station that was placed on the reference crop.

The Penman-Monteith equation requires the following parameters:

a. Minimum and maximum daily temperature.

b. *Relative humidity*. Depending on the availability of data, different equations are used. The data requirements are the following: (i) minimum and maximum daily relative humidity, (ii) maximum daily relative humidity or (iii) average daily relative humidity. In case where no humidity data are available, an estimation is required considering that the dew point temperatures are the same as the daily minimum temperatures.

c. *Solar radiation*. Different equations are used to consider the solar radiation. In order to calculate the solar radiation, if we do not access to the solar radiation directly we need (i) hours of sunshine per day or (ii) cloudiness fraction or the Hargreaves formula, based on minimum and maximum daily temperature and an adjustment coefficient (Krs) to estimate the solar radiation.

d. Wind speed. (An adjustment can be made if the wind speed measurement height has been previously measured).

e. Latitude and altitude of the climate measurement station.

f. The meteorological data measured and used in this study are mean daily air temperature (T_{mean}); maximum and minimum air temperature (T_{max} and T_{min}); mean daily relative humidity (RH); mean daily wind speed (u) and daily net radiation (R_n).

3. Results and discussion

3.1. Comparison between micrometeorological measurements and scintillometry

The comparison period for the ET measured by scintillometry and micro-meteorology measurements covered 2 months between July and August 2015, which included a range of climatic conditions to test the performance of the proposed scintillometry calculation method. The average air temperature was 23°C and ranged between a minimum of 9°C and a maximum of 32°C. The average ground temperature was 22°C and ranged between a minimum of 16°C and a maximum of 25°C. The C_n^2 measurements were made on a continuous time scale at 60 min intervals and averaged every 1 min and were synchronized with a weather station. R_n and G are calculated based on other meteorological data. Sensible heat fluxes with 60 min intervals were calculated using a step by step methodology provided by the method previously developed. The 60 min ET rates were computed as a residual from the energy balance equation, with calculated R_n and G fluxes and using an estimated H. **Figures 2** and **3** show the data acquired by the micro-meteorological station. **Figure 2** displays air and ground temperature measurements and, besides, the wind speed.

Figure 3 presents the measurements of humidity and pressure. All the data were acquired, at the same time, and stored by the electronic system. The measurements are detailed on a period of 7 days for simplicity of analysis. The air temperature was measured at a height of 0.3 m above the crop canopy and shows large variations between the maxima and minima. We calculate a ΔT around 15°C. The ground temperature was measured beneath the canopy foliage

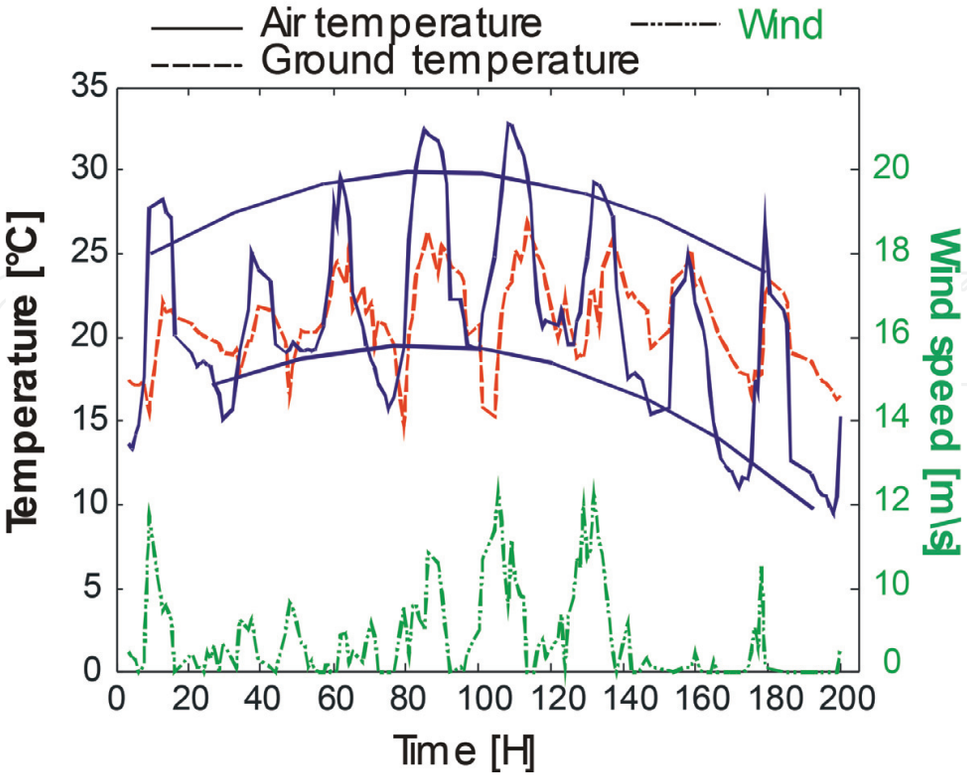


Figure 2. Measurements of air, ground temperature and wind during considered period. The lines give the average minimal and maximal air temperature.

with a sensor at 0.05 m underground. The ground temperature data show small amplitudes of variation with an average ΔT between the maximum and minimum of temperature around 5°C. The comparison between the two measured temperatures at two different heights shows a constant average value for the ground temperature and a limited variation of the average temperature with a maximum value of 25°C. It is interesting to note that the maximum of average air temperature value corresponds to the days where the wind is the maximum. The ground temperature is not sensible to the wind and account for the temperature changes with the canopy as shelter. The maximum in the average value for the air temperature corresponds also to the maximum of humidity. However, the atmospheric pressure is not related to the air temperature during the presented period of analysis. Based on the acquired micro-meteorological parameters and atmospheric turbulence measurements, evapotranspiration was calculated.

Figure 4 presents the comparison between the evapotranspiration data acquired with the scintillometer and the FAO-56 method during the same period of atmospheric parameter measurements. Differences are observed, in particular, during the night where the temperature falls. Those differences can be attributed to the few numbers of parameters used in the calculation with the FAO-56 method. The discrepancies between the two measurements of ET correspond to the maximum of humidity and minimum of wind. The variation between the two measurements can be checked in **Figure 5**, where the ETP computed using the FAO method regarding the ETP calculated with scintillometer data are plotted. A coefficient of

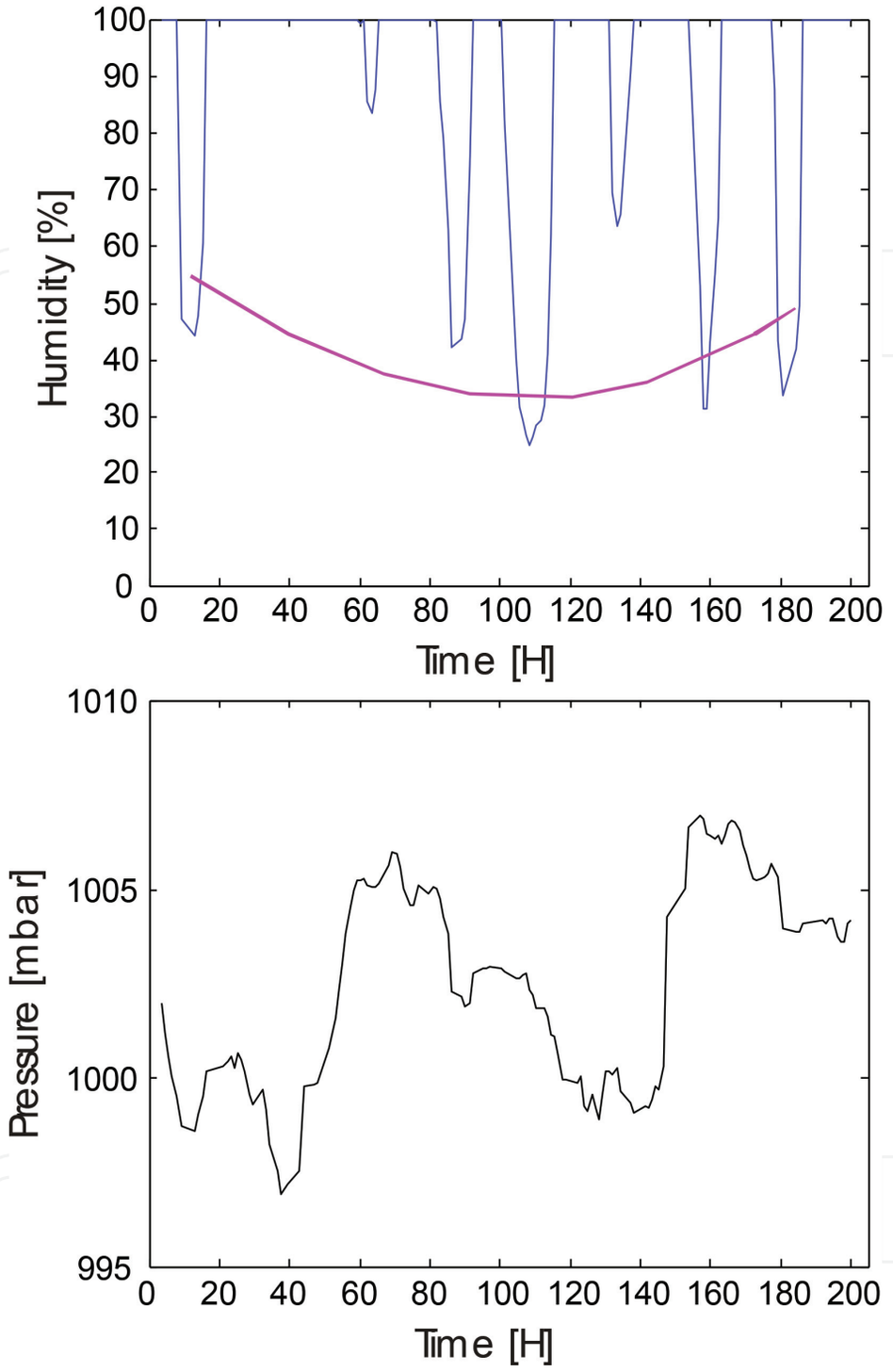


Figure 3. Measurement of the atmospheric humidity and pressure.

0.78 is found between the two methods meaning that $ETP_{FAO} = 0.78\ ETP_{scin}$. Therefore, the values are lower with FAO than with scintillometry and, consequently, evapotranspiration is underestimated. Note that the evapotranspiration measurement with scintillometry has proven being close to the data measured with Eddy-covariance [22, 23].

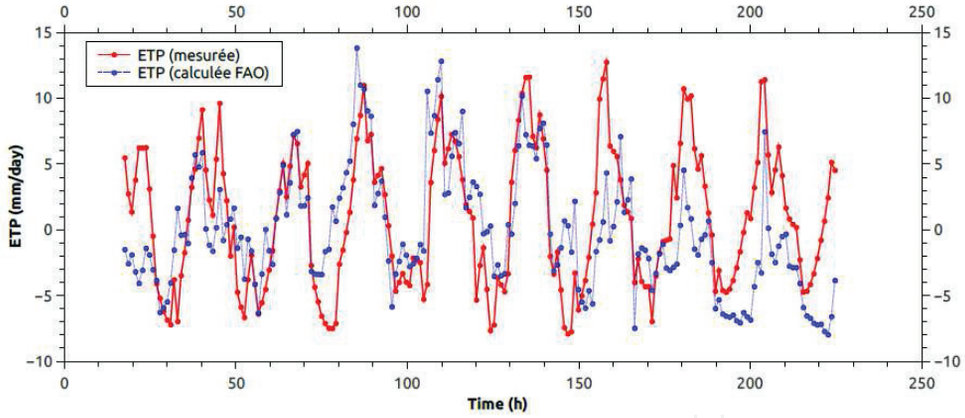


Figure 4. Comparison of the ET measured with the FAO-PM56 model based on the measurements of a limited number of parameters (T_{min}, T_{max}, T_{avg}, R_s) and scintillometric data.

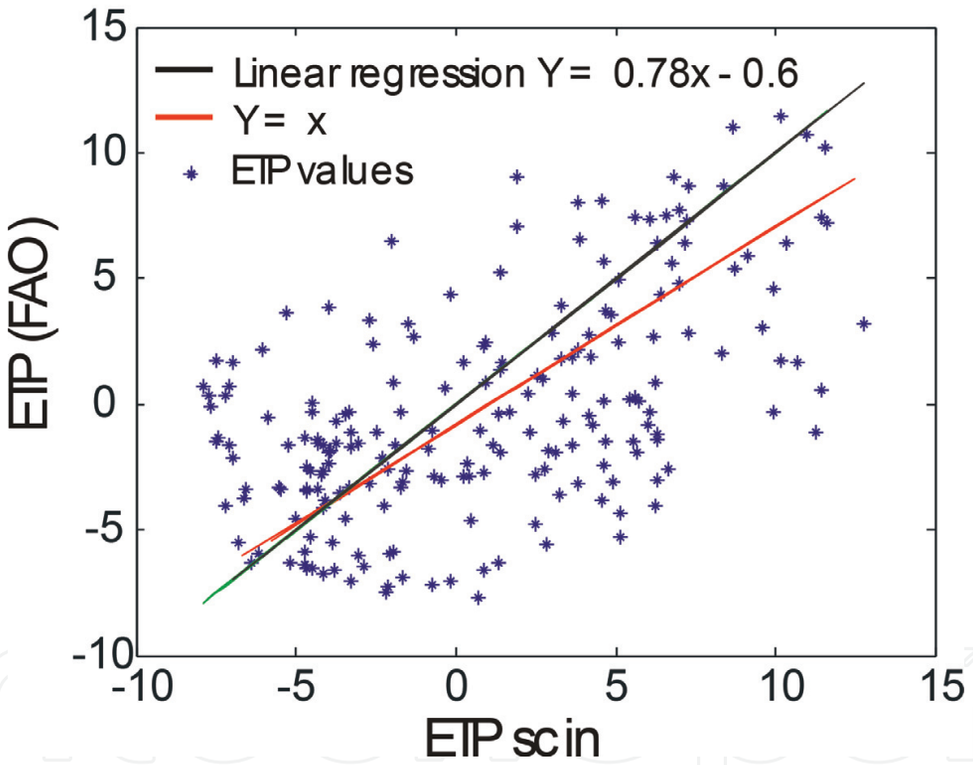


Figure 5. Comparison of the two measured ET data. The curves show the fitting points calculated with linear regression and the ideal curve representing a perfect similar relation of the two ET.

3.2. Influence of environmental parameters

In order to account the influence of the main meteorological parameters on the measurement sensibility of ETP, the effect of temperature variations is observed as the main influence on the measurements obtained by the FAO-56 and the scintillometer. Thus, the calculation is limited to temperature differences since scintillometer is more sensitive to small fluctuations of the refractive index of the air caused by those variations of temperatures.

Firstly, considering the ETP solution from a set of variable values (Eq. (8)) given by the FAO-56 where the dominant variable is the air temperature (T_A). Indeed, each term in Eq. (8) can be rewritten as a function of the temperature, thus

$$ET_0 = \frac{[0.408.\Delta R_n + \gamma.\frac{900}{(T_A+273)}\ .u_2.(e_s - e_s.H_D)]}{(\Delta + \gamma.\ (1 + 0.34.u_2))} \tag{9}$$

where u_2 is the wind speed and H_D is the relative humidity. R_n, e_s, γ and Δ are depending on T_A (see Appendix A).

The dominant variable value is fluctuated by a small amount while keeping all other values constant, and we note the change of the solution. The goal is to determine how sensitive the output calculation of evapotranspiration could be with respect to the calculation elements which are subject to uncertainty of variability.

Figure 6 shows that a variation of ±0.5°C of T_A leads to a small variation of ET_0 (±1.3 mm/day) with the FAO method. However, a variation of ±0.5°C leads to a variation of ±2.2 mm/day with the scintillometric method. Therefore, the scintillometer method is more sensitive to fluctuations of air temperature. This is not a novelty because small fluctuations of air temperature induce random variations in the refractive index of the turbulent atmosphere by changing the intensity of turbulence C_n^2. The propagation distance enhances any fluctuations of the laser beam. Moreover, it was shown that the C_n^2 can be measured with a good precision [24]. According to this result, a sensitivity analysis based on the analytical calculations was conducted.

The approach consists in mathematically differentiate the equation under study to derive equations for the change rate of the independent variable with respect to each dependent variable. The sensitivity for the air temperature is calculated applying the PM FAO-56 method. The ET_0 is considered as a function with multi-variables v_1, v_2, v_3, …, as $ET_0 = f(v_1, v_2, v_3, \ldots)$ with $v_1 = T_a$, $v_2 = R_n$, $v_3 = u_2$ and so on. The sensitivity equation can be developed by

$$ET_0 + \Delta ET_0 = f(v_1 + \Delta v_1, v_2 + \Delta v_2,\ v_3 + \Delta v_3,\ \ldots)\ . \tag{10}$$

After applying the Taylor's theorem and considering only the first order, the expression yields

$$\Delta ET_0 = \frac{\partial ET_0}{\partial v_1}\Delta v_1 + \frac{\partial ET_0}{\partial v_2}\Delta v_2 + \frac{\partial ET_0}{\partial v_3}\Delta v_3 + \ldots \tag{11}$$

The P–M method is a multi-variable model. Several variables have different dimensions and various ranges of values, which makes it difficult to compare the sensitivity by partial derivatives. The partial derivative is transformed into a non-dimensional form.

The substitution of the relative forms, $(ET_0)_{rel} = (\Delta ET_0/ET_0)$ and $v_{rel} = \Delta v/v$ for each variable, yields

$$(ET_0)_{rel} = (\Delta ET_0/ET_0) = \left(\frac{\partial ET_0}{\partial v_1}\frac{v_1}{ET_0}\right)\frac{\Delta v_1}{v_1} + \left(\frac{\partial ET_0}{\partial v_2}\frac{v_2}{ET_0}\right)\frac{\Delta v_2}{v_2} + \left(\frac{\partial ET_0}{\partial v_3}\frac{v_3}{ET_0}\right)\frac{\Delta v_3}{v_3} + \ldots \tag{12}$$

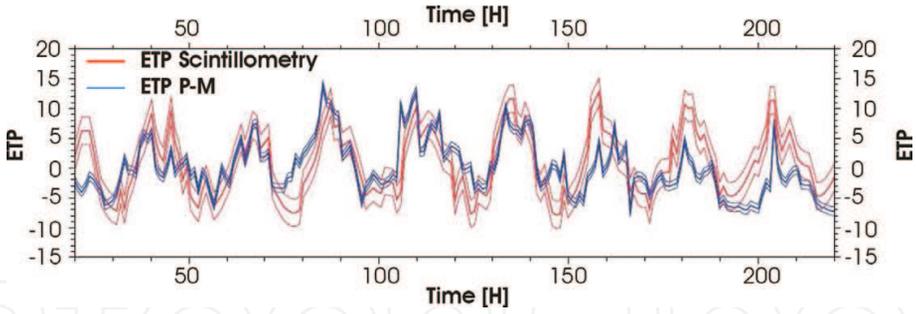


Figure 6. Comparison of the influence of a small variation of temperature (± 0.5°C) on the two methods of measurements of ET.

where Sv_i is called the sensitivity coefficient and it is equal to $\frac{\partial ET_0}{\partial v_i}\frac{v_i}{ET_0}$ for the variable v_i. This term becomes a dimensionless coefficient which expresses the percentage of the relative variable change transmitted to the relative dependent variable. Basically, a positive/negative sensitivity coefficient of a variable indicates that ET_0 will increase/decrease as the variable increases. The bigger the sensitivity coefficient, the larger the effect a given variable has on ET_0. A sensitivity coefficient Sv_i of 0.2 would show that a 10% change in v1 ($\Delta v_1/v_1 = 0.10$) would cause a 2% change in ET_0 ($\Delta ET_0/ET_0 = 0.02$) if $(ET_0)_{rel}$ is dependent of the relative change $\Delta V_1/V_1$ in Eq. (12) [25].

The partial derivatives needed for the determination of the sensitivity coefficient S_{TA} corresponding to the influence of air temperature:

$$S_{TA} = \lim_{\Delta T_A \to 0}\left(\frac{\frac{\Delta ET_0}{ET_0}}{\frac{\Delta T_A}{T_A}}\right) = \frac{\partial ET_0}{\partial T_A}\cdot\frac{T_A}{ET_0} \tag{13}$$

The calculation is done analytically by means of symbolic calculation of Mathematica (Wolfram) in Appendix A. It found a sensitivity coefficient value of 0.12 for the maximum measured temperature of 32.8°C, a humidity of 24.7%, a wind measurement of 3.9 m/s, an evapotranspiration of 10.4 mm/day and an atmospheric pressure of 1002 mbar.

This sensitivity obtained for the FAO-56 measurement and the one given by the scintillometer is compared. For the latter instrument, based on optical metrology, the intensity fluctuations of visible beams are more sensitive to temperature fluctuations than humidity fluctuations.

In the displaced-beam scintillometer measurements, the path-averaged measurements of C_n^2 are obtained. Additional measurements have separately carried out including temporally averaged pressure, air temperature, humidity, as well as the height of the beam above the field and the Bowen ratio. All those sources of measurements contain uncertainties. Uncertainty is propagated from the measured parameters to the derived variables through the set of equations employed and written previously (Eq. (1)–(7)). Different scintillometer sensitivity studies have been done. One of them uses the Monte-Carlo error analysis [26] and shows that the experimental coupling of inertial-dissipation methods is promising, since the propagation of statistical errors in the acquired parameters to the final value is limited. Those methods are based on measurements of the structure parameters of momentum, temperature and humidity

with optical methods leading to the calculation of the momentum flux and the heat flux. Another study [27] calculates the relative uncertainty of the friction velocity u* or turbulence velocity scale. The goal was to know how precisely the measurement of the friction velocity u* can be done by using a path-averaged optical propagation. The conclusion is that the measurement of the inner scale of turbulence (λ_o) contributes to the largest uncertainty and must be done precisely. A recent study analyses the impact of the Bowen ratio on the flux value and uncertainty [28]. It is shown that the Bowen ratio has a large impact on the accuracy of C_T^2 and on the sensible heat flux estimation in the case of strong humidity conditions ($\beta < 1$). A $\beta > 1$ was registered during the summer experiment. A relative uncertainty is estimated on the measurements, considering only the temperature with the scintillometer and following the procedure described for remote sensing [29]

$$\frac{\Delta ET_0}{ET_0} = \left(\frac{\Delta T_A}{T_A}\right) S_{T_A}. \tag{14}$$

The following tolerances used to estimate uncertainties have been taken:

Quantities	Unit	Assumed standard deviation
Temperature	°C	±1°C (−20–0°C)
		± 0.5°C (0–40°C)
		± 1°C (40–60°C)
Wind speed	$m.s^{-1}$	± 0.5 m/s (0–20 m/s)
		± 3% (20–60 m/s)
Humidity	%	± 2% (0–90%)
		± 3% (90–99%)
		Temperature dependence
		± 0.05% RH°C^{-1}
Atmosphere pressure	Pa	± 50 Pa (300–1100 hPa)
Path length	m	± 3
Path height	m	0.2
C_n^2	$K^2.m^{-2/3}$	± 0.5%

A value of 0.05 is found for the scintillometer sensitivity corresponding to sensitivity 2.4 lower than the FAO-56 sensitivity.

The main factor of uncertainty comes from the measurement of C_n^2. The scintillometer uncertainty is lower than the FAO-56 uncertainty.

3.3. Neural network for estimating evapotranspiration

Several researchers have used artificial neural network (ANN) models to estimate or forecast evapotranspiration as a function of micro-meteorological data [30, 31]. Neural networks are

an information processing technique based on a biologically-inspired programming paradigm, such as the brain enabling computer softwares to learn from observational data. The similarity with the human brain consists in the following characteristics: (i) a neural network acquires knowledge or informations through a process of learning; (ii) a neural network's knowledge is stored within inter-neuron connection strengths known as synaptic weights. In a feed-forward ANN model, a neuron performs two functions; it sums the weighted inputs from several connections and then applies a nonlinear function to the sum. The resulting value is propagated through outgoing connections to other neurons. The neurons or interconnection points are arranged in layers. The input layer receives data as inputs from real data acquisition; succeeding layers receive weighted outputs from the preceding layer as inputs, and the last layer gives the final results. ANNs are trained using a training algorithm and a training data set to adjust the connection weights, which result in an ANN model that can generate the most similar output vector to the target vector [32]. It is important to note that in most of the papers, different ANN models are considered including the generalized feedforward (GFF), linear regression (LR), multi-layer perceptron (MLP) and probabilistic neural network (PNN) [33].

The most common neural network model is the multi-layer perceptron (MLP). The MLP and many other neural networks learn using an algorithm called backpropagation artificial neural networks (BPANN). With backpropagation, the input data are repeatedly presented to the neural network. As soon as the calculation is done, the obtained result at the final layer of the neural network is compared to the desired output, and an error is calculated. This error is then fed back (backpropagated) to the neural network input layer and used to adjust the synaptic weights such that the error decreases with each iteration. Finally, the neural model of synaptic connections converges closer and closer to the desired output. These calculations with feedbacks are known as "training."

The objective of this study was to test BPANN models for forecasting daily ET_O with input data based on minimum meteorological data, considering the mean for maximum and minimum air temperatures and extraterrestrial radiation for the FAO-PM56 and scintillometry model for finally to compare them. The comparisons were based on statistical differences during a period of measurements with forecasted data by a set of measured data as input parameters and compared to data measured using FAO-PM56 or scintillometry daily ET_O values as references.

Firstly, the FAO-PM56 method was used to calculate daily ET values from climatic data. The ET data were then used to train and test the ANN model. 120 h are considered corresponding to 5 days as training data. Secondly, evapotranspiration data based on the scintillometer data were used to train and test the ANNs model. The same number of days is kept as input data.

Figure 7(a) shows the plot of the predicted data as a function of the measured data for scintillometry. A shift in the plot of the predicted values for the input data acquired with the scintillometry method is seen. However, the predicted data follow the measured data variations. The slope of the fitting curve is 0.76 close to the perfect value of 1 in the case of similar values between the predicted and measured data (**Figure 7c**). With FAO-PM-56

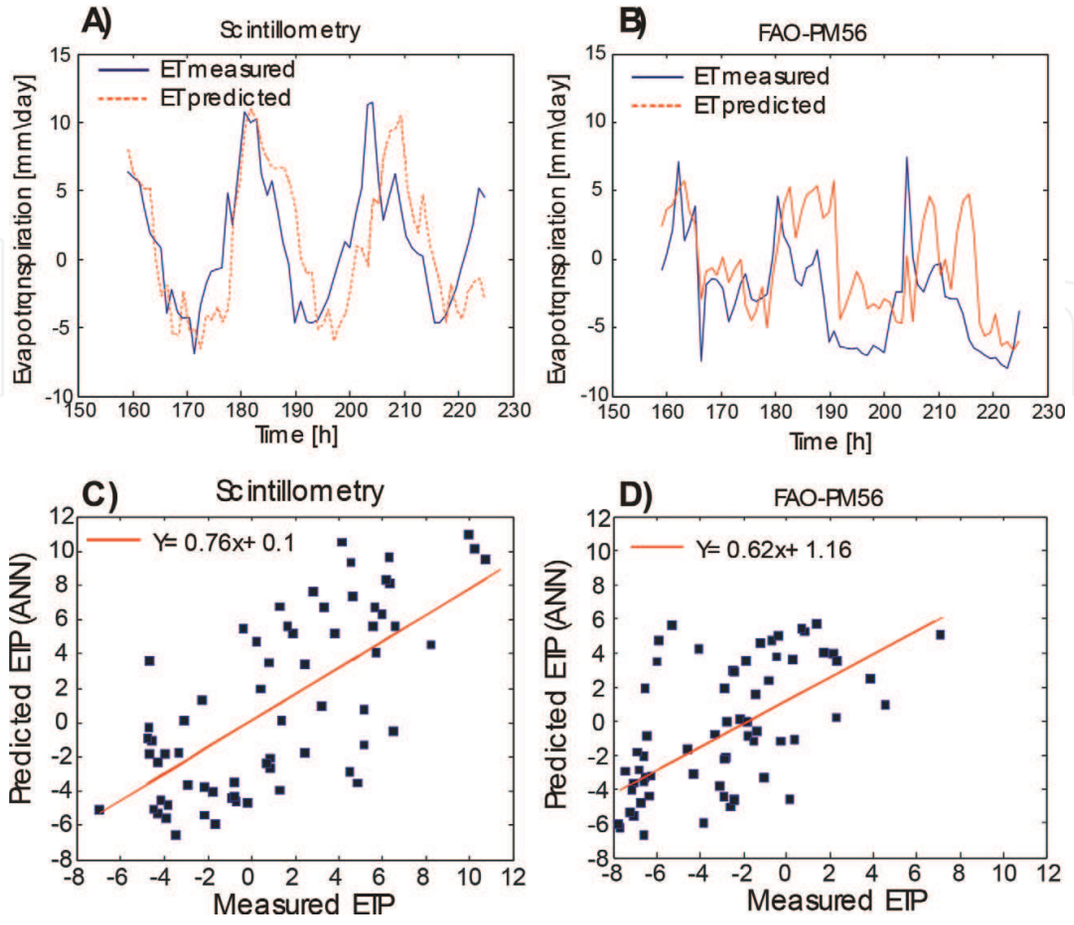


Figure 7. Predicted values of ET based on two different input training data of ET one with FAO-PM56 and the other one with scintillometric data. The calculation is done with an artificial neural network (ANN).

data, the BPANN calculations show that the predicted values have no time shift but large differences in intensity (**Figure 7b**). (**Figure 7d**) presents the corresponding plot of the predicted values as a function of the measured values. The slope is 0.62 meaning that the predicted values are almost close to twice the measured values. The comparison between the two predicted values is presented in **Figure 8** where the plot of the two calculations with the ANN model shows a slope of 1.5 demonstrating the big difference in the obtained values of ET. As a conclusion, the scintillometry data are better input values for the forecasting of ET.

In order to know if the difference in the final results of the predicted values done with the ANN model comes from the capacity to sufficiently have training data, the difference between the predicted and measured values as a function of the number of days of input data is calculated. **Figure 9** displays the optimum values. It is observed that up to 2.5 days of forecasting, there is no difference between the two methods of evapotranspiration calculations. Nevertheless, after 2.5 days, the evapotranspiration calculation with the scintillometer shows constant values in the difference between measured and predicted scintillometric input data. This is not the case with FAO-PM56 where the difference between predicted and measured data increases. The scintillometry is more able to predict for more days than the FAO-PM56

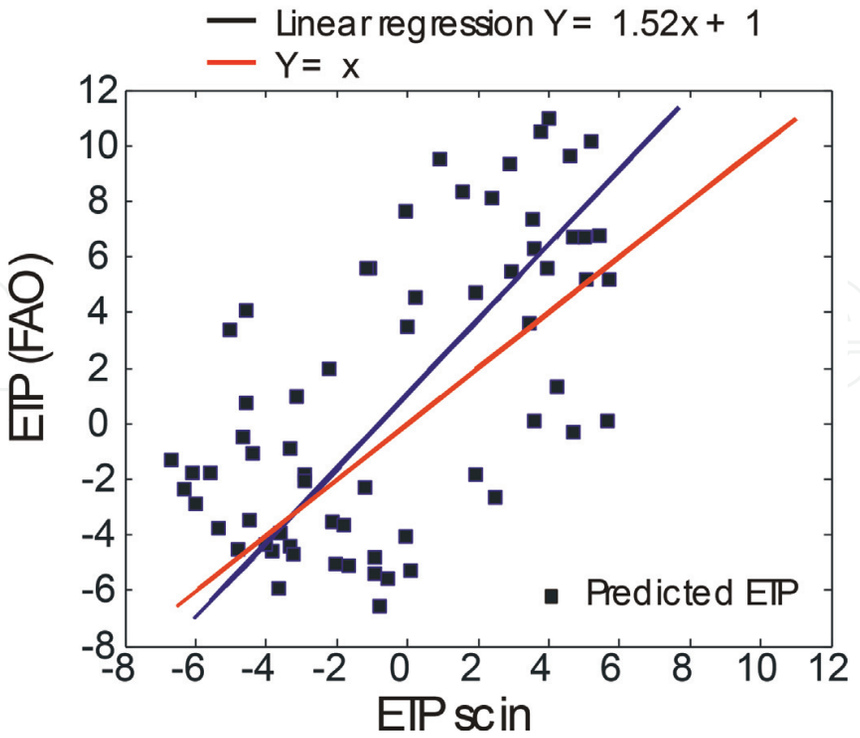


Figure 8. Comparison of the two sets of forecasted values with an artificial neural network. The curves show the fitting points and the ideal case of similar values.

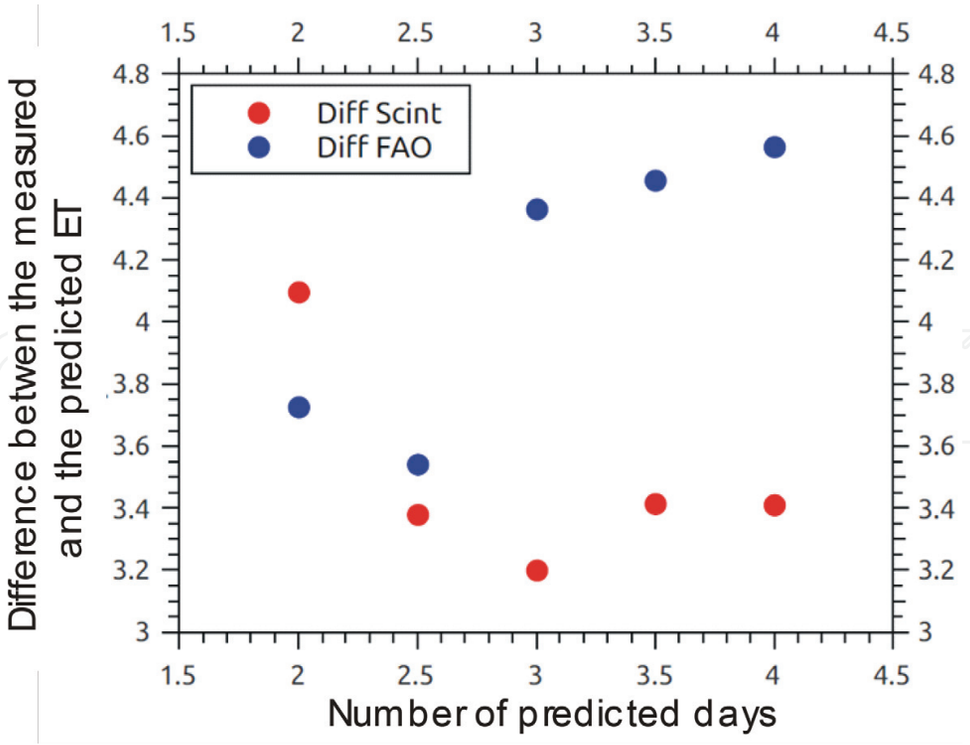


Figure 9. Calculation of optimal forecasted days as a function of the number of input training days in the ANN calculation for two different methods of ET measurements.

method. This result can be explained by the low propagation of small variations or errors in the calculation of ET using the scintillometer method. However, in the FAO-PM56 method with few input variables, small variations in the parameters for the calculation of ET lead to larger uncertainties.

4. Conclusion

Two methods to acquire ET from a crop field (Maize) are presented. One of them is based on atmospheric turbulence data acquired with a laser beam scintillometric method and another one is based on the calculation with limited meteorological data using the FAO-PM56 method. The comparison between the two ET measurements shows a difference in the final result. The measurements with micro-meteorological parameters are lower than with scintillometric parameters leading to an underestimation of the real ET. This is an important result because farmers must accommodate in advance their crop water demand to irrigation requirements. An overestimation of ET can lead to a deficit of irrigation water, and on the contrary, a low estimation of ET can lead to water waste. The measurements have shown a lower measured value of ET with the FAO-PM56 method. Moreover, the FAO-PM56 method for obtaining ET is more sensible to a small error in the acquisition of the temperature. Then, while the scintillometer measurements are representative of the turbulent fluctuations along the whole beam path, the FAO-PM56 measurements are typically representative measurements of localized areas near the respective different meteorological acquisition instruments.

Finally, using artificial neural network, evapotranspiration forecast for short-term near-future is obtained. In addition, it is presented results for two different input training data, and it is showed that evapotranspiration data based on scintillometric data acquisition are more reliable for forecasting. An optimum value was found in the number of days of training data to obtain the best forecast. In this case also, evapotranspiration with scintillometric data increases the number of predicting reliable days.

Appendix A. Supplementary data

ETP solution from a set of variable values with a Mathematica script:

```
et[TA_, WD_, HD_, RS_, H_, DAY_, Y_, LAT_] :
= (0.408*(4098*( 0.611*Exp[17.27*TA/(TA + 237.3)])/(TA
  + 237.3)^2)*((0.77*RS) - ((4.903*10^(-9)*(TA + 273)^4
  *(0.34 - 0.14*Sqrt[( 0.611*Exp[17.27*TA/(TA + 237.3)])*HD]))
  *(1.35*(Min[RS/((0.75 + 0.00002*H)
  *(24*60/Pi*(0.0820)*(1 + 0.033*Cos[2*Pi * DAY/Y])
  *((\[Pi]/2 - ArcTan[(-Tan[(3.14/180*LAT)]*Tan[(0.409*Sin[2*\[Pi]
  *DAY/Y - 1.39])])/(Max[1 - Tan[(3.14/180*LAT)]^2*
```

```
Tan[(0.409*Sin[2*Pi * DAY/Y - 1.39])]^2 , 0.00001])^0.5])
*Sin[(3.14/180*LAT)]*Sin[(0.409*Sin[2*Pi * DAY/Y - 1.39])]
+Cos[(3.14/180*LAT)]*Cos[(0.409*Sin[2*Pi * DAY/Y - 1.39])]
Sin[(Pi/2 - ArcTan[(-Tan[(3.14/180*LAT)]*Tan[(0.409
*Sin[2*Pi * DAY/Y - 1.39])])/(Max[1 - Tan[(3.14/180*LAT)]^2
*Tan[(0.409*Sin[2*Pi * DAY/Y - 1.39])]^2 , 0.00001])^0.5])])))), 1]) - 0.35)))
+(0.00163*(101.3*((TA + 273 - 0.0065*H)/(TA + 273))^5.26)/
(2.501 - (0.002361)*TA))*900/(TA + 273)*WD*((0.611
*Exp[17.27*TA/(TA + 237.3)]) - (0.611*Exp[17.27
*TA/(TA + 237.3)])*HD))/((4098*(0.611*Exp[17.27*TA/(TA
+237.3)])/(TA + 237.3)^2) + ( 0.00163*(101.3*((TA + 273 - 0.0065*H)/
(TA + 273))^5.26)/(2.501 - (0.002361)*TA))
*(1 + 0.34*WD));
```

Author details

Antonin Poisson[1], Angel Fernandez[1,3], Dario G. Gomez[2], Régis Barillé[1]* and Benoit Chorro[4]

*Address all correspondence to: regis.barille@univ-angers.fr

1 MOLTECH-Anjou, University of Angers, Angers, France

2 Instituto de Física, Pontificia Universidad Católica de Valparaíso, Valparaíso, Chile

3 Departamento de Física, Universidad Técnica Federico Santa María, Valparaíso, Chile

4 Océalia, CIVRAY, France

References

[1] Intergovernmental Panel on Climate Change. Synthesis Report. 2014. https://www.ipcc.ch/report/ar5/

[2] Dasa B, Singha A, Pandaa S N, Yasuda H. Optimal land and water resources allocation policies for sustainable irrigated agriculture. Land Use Policy. 2015;**42**:527–537

[3] Abtew W, Melesse A. Evaporation and Evapotranspiration. Berlin, Heidelberg: Springer-Verlag; 2013

[4] Béziata P, Rivallanda V, Tallec T, Jarosza N, Bouleta G, Gentine P, Ceschia E. Evaluation of a simple approach for crop evapotranspiration partitioning and analysis of the water budget distribution for several crop species. Agricultural and Forest Meteorology. 2013;**177**:46–56

[5] Pereira L, Allen R G, Smith M, Raes D. Crop evapotranspiration estimation with FAO56: Past and future. Agricultural Water Management. 2013;**147**:4–20

[6] Verstraeten W W, Veroustraete F, Feyen J. Assessment of evapotranspiration and soil moisture content across different scales of observations. Sensors. 2008;**8**:70–117

[7] Beyrich F, Bange J, Hartogensis O K, Raasch S, Braam M, van Dinther D, Gräf D, van Kesteren B, van den Kroonenberg A C, Maronga B, Martin S, Moene AF. Towards a Validation of Scintillometer Measurements: The LITFASS-2009 Experiment. Boundary Layer and Mesoscale Meteorology. 2012;**144**:83–112

[8] Meireles MRG, Almeida PEM, Simões MG. A Comprehensive Review for Industrial Applicability of Artificial Neural Networks, IEEE Trans. Indust. Elec. 2003;**50**(3): 585–601

[9] Gardner MW, Drorling SR. Artificial neural networks (the multilayer perceptron)—A review of applications in the atmospheric sciences. Atmospheric Environment. 1998;**32 (**14/15):2627–2636

[10] Kleissl J, Gomez J, Hong SH, Hendrickx JMH, Rahn T, Defoor WL. Large Aperture Scintillometer Intercomparison Study. Boundary Layer and Mesoscale Meteorology. 2008;**128**(1):133–150

[11] Chehbouni A. Estimation of heat and momentum fluxes over complex terrain using a large aperture scintillometer. Agricultural and Forest Meteorology. 2000;**105**:215–226

[12] Hill RJ. Algorithms for obtaining atmospheric surface-layer fluxes from scintillation measurements. Journal of Atmospheric and Oceanic Technology. 1997;**14**:456-467

[13] Cammalleri C, Agnese C, Ciraolo G, Minacapilli M, Provenzano G, Rallo G. Actual evapotranspiration assessment by means of a coupled energy/hydrologic balance model: Validation over an olive grove by means of scintillometry and measurements of soil water contents. Journal of Hydrology. 2010;**392**:70–82

[14] Zhang X, Jia X, Yang J, Hua L. Evaluation of MOST functions and roughness length parameterization on sensible heat flux measured by large aperture scintillometer over a corn field. Agriculture and Forest Meteorology. 2010;150:1182–1191

[15] Odhiambo GO, Savage MJ. Surface layer scintillometry for estimating the sensible heat flux component of the surface energy balance. South African Journal of Science. 2009;**105**:208–216

[16] de Bruin HAR. Analytic solutions of the equations governing the temperature fluctuation method. Boundary Layer and Mesoscale Meteorology. 1994;**68(**4):427–432

[17] Subedi A, Chávez J L, Crop Evapotranspiration (ET) Estimation Models: A Review and Discussion of the Applicability and Limitations of ET Methods, Journal of Agricultural Science. 2015;**7**(6): 50–68.

[18] Novák V. Methods of Evapotranspiration Estimation', Evapotranspiration in the Soil-Plant-Atmosphere System, Progress in Soil Science. 2012; editor Springer Netherlands, 165–215

[19] Rivasa R, Caselles V: A simplified equation to estimate spatial reference evaporation from remote sensing-based surface temperature and local meteorological data. Remote Sensing of Environment. 2004; **93**:68–76

[20] Droogers P, Allen R G: Estimating reference evapotranspiration under inaccurate data conditions, Irrigation and Drainage Systems. 2002; **16**:33–45

[21] McMahon T A, Peel M C, Lowe L, Srikanthan R, McVicar T R: Estimating actual, potential, reference crop and pan evaporation using standard meteorological data: A pragmatic synthesis, Hydrology and Earth System Sciences Journal. 2013; **17**:1331–1363

[22] Allen R G, Pereira L S, Raes D, Smith M: Crop evapotranspiration: guide lines for computing crop water requirements, FAO irrigation and Drainage, Paper No. 56. 1998; FAO: Rome, Italy

[23] Hoedjes J C B, Chehbouni A, Ezzahar J, Escadafal R, De Bruin H A R: Comparison of Large Aperture Scintillometer and Eddy Covariance Measurements: Can Thermal Infrared Data be used to capture footprint-induced differences, Jopurnal of Hydrometeor. 2007; **8**:144–158

[24] Wang T, Ochs G R, and Clifford S F: A saturation-resistant optical scintillometer to measure C_n^2, JOSA. 1978; **68**:334–338

[25] Liu SM, Xu ZW, Zhu Z L, Jia Z Z, Zhu M J, Measurements of evapotranspiration from eddy-covariance systems and large aperture scintillometers in the Hai River Basin, China, Journal of Hydrology. 2013; **487**:24–38

[26] Saxton K E: Sensitivity analyses of the combination evapotranspiration equation, Agricultural Meteorology. 1975; **15**:343–353

[27] Moroni C, Navarra A, Guzzi R: Estimation of the turbulent fluxes in the surface layer using the inertial dissipative method: A monte-carlo error analysis, Boundary Layer and Mesoscale Meteorology. 1990; 50:339–354

[28] Andreas E L: Uncertainty in a path-averaged measurement of the Friction Velocity u*, Journal of Applied Meteorology and Climatology. 1992; **31**:1312–1321

[29] Ustinov E A: Sensitivity Analysis in Remote Sensing, Springer Briefs in Earth Sciences, Springer. 2015

[30] Govindaraju R S, Rao A R: Artificial Neural Networks in Hydrology, Kluwer Academic Publishers, Amsterdam. 2000

[31] Traore S, Luo Y, Fipps G: 'Deployment of artificial neural network for short-term forecasting of evapotranspiration using public weather forecast restricted messages', Agricultural Water Management. 2016; **163**:363–379

[32] Falamarzi Y, Palizdan N, Feng Huang Y, Lee T S: Estimating evapotranspiration from temperature and wind speed data using artificial and wavelet neural network (WNNs), Agricultural Water Management. 2014; **140**:26–36

[33] Yassina M A, Alazbaa A A, Mattar M A: Artificial neural networks versus gene expression programming forestimating reference evapotranspiration in arid climate, Agricultural Water Management. 2016; **163**:110–124

IntechOpen

IntechOpen